Virioplankton and picoplankton abundance and spatial distribution in Tawi-Tawi's shallow waters: A snapshot amidst northeast monsoon conditions

Edcel R. Sudaria[1], Gency L. Guirhem-Helican[1], Richard N. Muallil[2], Charina Lyn Amedo-Repollo[3], Cristy S. Acabado[1]*

[1]Institute of Marine Fisheries and Oceanology, College of Fisheries and Ocean Sciences, University of the Philippines Visayas, Miagao, Philippines 5023

[2]Mindanao State University - Tawi-Tawi College of Technology and Oceanography, Sanga-Sanga, Bongao, Tawi-Tawi, Philippines 7500

[3]Marine Science Institute, College of Science, University of the Philippines Diliman, Quezon City, Philippines, 1101

ABSTRACT

This study examines the environmental conditions and hydrographic dynamics in Tawi-Tawi within the Sulu Archipelago, a region influenced by the interplay of distinct water masses from the cooler, saltier Sulu Sea and the warmer, fresher Celebes Sea. Pronounced spatial gradients in sea surface temperature and salinity were observed; however, these hydrographic patterns did not correlate directly with Chl *a* concentrations or microbial plankton biomass, indicating that biological productivity is more strongly governed by current velocity and tidal dynamics. Spectral analysis confirmed tidal currents as the dominant driver of water transport, explaining over 95% of the variability in the region. Tidal currents can induce horizontal advection and retention zones on the shallow (<200 m) bathymetric shelves around Bongao, Sibutu, and Sitangkai, which promote plankton aggregation and enhanced nutrient mixing. Baroclinic tides were generated by the interaction of barotropic tides with complex bathymetry, such as in Sibutu and Sitangkai. This interaction produces internal waves that support vertical nutrient flux and persistent upwelling, enriching surface waters as evidenced by elevated Chl *a* and microbial density in Tawi-Tawi. Sampling during highest high water further intensified vertical mixing, nutrient availability, and horizontal advection, collectively elevating picoplankton and virioplankton abundance. The microbial community was dominated by viruses and heterotrophic bacteria, but *Synechococcus* prevailed among the autotrophs due to its high adaptability to dynamic mixing conditions. The spatial heterogeneity in microbial populations reflects the combined influence of physical transport processes and the ecological tolerances of plankton, underscoring the complexity of biological productivity regulation in this archipelagic system.

KEYWORDS:

Tawi-Tawi; Hydrography; Tides; Flow cytometry; Plankton

INTRODUCTION

The Tawi-Tawi Islands are geographically situated at the southernmost tip of the Philippines, forming an integral part of the Sulu Archipelago. It is strategically positioned between the Sulu Sea to the north and the Celebes Sea to the south, sharing sea borders with Malaysia and Indonesia. This region is known for its complex oceanography, including strong currents and deep trenches. The water exchange between the Sulu and Celebes Seas is facilitated through the shallow sill in the Sibutu Passage with a sill depth of ~245 m (Gordon et al., 2012). Regionally, both the Sulu and Celebes Seas exhibit thick barrier layers (i.e., >36 m) below the mixed layer depth in the water column, hindering vertical mixing of heat, nutrients, and other particles (Chu et al., 2002). The barrier layer prevents vertical mixing from the deeper, nutrient-rich waters to the mixed layer depth, creating an oligotrophic environment that facilitates pico- and virioplankton growth (Bouman et al., 2011; Li, et al. 2023). Tawi-Tawi, thus, presents an interesting hydrographic setting that is deemed to be explored.

Corresponding Author:
Institute of Marine Fisheries and Oceanology, College of Fisheries and Ocean Sciences, UP Visayas, Miagao; email address: csacabado@up.edu.ph

In the Sulu Sea, the northeast monsoon is generally associated with an increase in marine productivity. Studies indicate that this period typically sees higher concentrations of surface chlorophyll *a* (Chl a) and corresponding lower sea surface temperatures (Acabado & Campos, 2018; Wang et al., 2006). The timing of this study, February, is particularly relevant as it falls within the mid-phase of the northeast monsoon season. This seasonal wind pattern is known to drive specific circulation and mixing processes, such as upwelling and intense water flow, that can significantly affect nutrient availability and, consequently, primary productivity. The resulting influx of cold, deep, nutrient-rich water provides the necessary inorganic resources (i.e., nitrate) that fuel the productivity peaks during the monsoon. Picoplankton are crucial during these peaks because their small size gives them a large surface-area-to-volume ratio, allowing them to rapidly and efficiently assimilate the sudden, high concentrations of upwelled nutrients (Chisholm, 1992). This superior efficiency in nutrient uptake allows picoplankton, which often dominate in warm, oligotrophic conditions, to respond quickly to the episodic nutrient enrichment and contribute a major fraction of the overall new primary production. This study provides a snapshot of the most abundant photosynthetic group in aquatic environments, planktonic organisms with <2 µm cell size, which play a crucial role as primary producers.

In the Philippines, semi-diurnal tides are prevalent in the Pacific Ocean, while diurnal tides are more common in the West Philippine Sea (Amedo-Repollo et al., 2021). For small islands and shallow coastal areas like Tawi-Tawi, the tidal frequencies (diurnal, semi-diurnal, and mixed), horizontal advection (flood and ebb), and vertical oscillations (barotropic and baroclinic) play a significant role in shaping marine productivity by enhancing nutrient input into surface waters (Baker, 2007; De Falco et al., 2022; Kossack et al., 2023; Stewart, 2008). Tidal currents flowing from the deep Celebes Sea to the shallow Sulu Archipelago generate internal tides propagating towards the Sulu Sea (Jackson et al., 2011). The vertical mixing of the water column induced by tide-bathymetry interaction drives the formation of cold fronts and localized upwelling (Jing et al, 2012). The persistent upwelling results in the formation of productivity hotspots in the region as indicated by elevated Chl a concentration (Takeda et al., 2007), which is potentially dominated by microplankton constituents (e.g., diatoms and dinoflagellates). In contrast, smaller plankton constituents such as picoplankton and virioplankton are often sparse and understudied in productive upwelling regions of the Philippines (Collado-Fabri et al., 2011).

Virioplankton (femtoplankton; <0.2µm) and picoplankton (0.2 - 2µm) are highly abundant in aquatic environments, but they have been relatively understudied. They are estimated to constitute a substantial portion of the total ocean biomass, contributing approximately 70% to 90% (Massana, 2011). Viruses in the ocean infect and lyse bacterial hosts, releasing cell contents and nutrients that become readily available for other organisms. On the other hand, picoplankton, a diverse group of microscopic organisms, are fundamental to marine ecosystems globally. This group encompasses the autotrophic components, such as picocyanobacteria (e.g., *Prochlorococcus*, *Synechococcus*) and picoeukaryotes, as well as heterotrophic prokaryotes, i.e., bacteria (Marie et al., 1997). Their ecological importance extends far beyond their role as primary producers. Picoplankton are responsible for nearly all photosynthesis occurring in the ocean and are crucial in the cycling of essential chemical elements, including carbon, nitrogen, phosphorus, and oxygen (Grob et al., 2007; Jiao et al., 2005). Given their foundational role in marine food webs and their known sensitivity to environmental changes, picoplankton are exceptionally valuable indicators of ecosystem health and productivity.

This study aims to describe the abundance and spatial distribution of picoplankton in the shallow coastal waters around three Tawi-Tawi Islands, namely Bongao, Sibutu, and Sitangkai. To do this, the relationship between *in-situ* picoplankton abundance and corresponding satellite-derived data of temperature, salinity, historical tidal sea level, and Chl a concentrations will be analyzed. Overall, it aims to contextualize these picoplankton observations within the prevailing oceanographic conditions, specifically considering the interplay of tidal forcing, bathymetry, and the potential localized environmental factors.

MATERIALS AND METHODS

Study site and sampling locations

The Sulu Archipelago waters are composed of the Sulu Sea in the north and the Celebes Sea in the south. The coastal waters around the islands of Tawi-Tawi are predominantly shallow, typically less

than 200 meters deep (Fig. 1A). The chain of small islands along the Sulu Archipelago provides a shallow bathymetry in the boundary between the Sulu Sea and the Celebes Sea (Fig. 1A). Bongao, Sibutu, and Sitangkai Islands are located at 5.029° N, 119.773° E; 4.767° N, 119.467° E; and 4.660 ° N, 119.400° E. A total of 18 stations were sampled for picoplankton, with six stations located around each of the islands of Bongao, Sibutu, and Sitangkai (Fig. 1B-C). Sampling stations are labeled as SB1 - SB6 (Sibutu), SIT1 - SIT6 (Sitangkai), and BOG1 - BOG6 (Bongao; Fig. 1B-C). All samples were collected during daytime high tides in a neap tide period on February 19-21, 2025. The bathymetric data used were obtained from the General Bathymetric Chart of the Oceans (GEBCO 2023 Grid; DOI: 10.5285/6364bd46-1c0e-1c4c-e053-6c86abc0c6c5). The spatial resolution of the said data is 15-arc second or approximately equal to ~500 m.

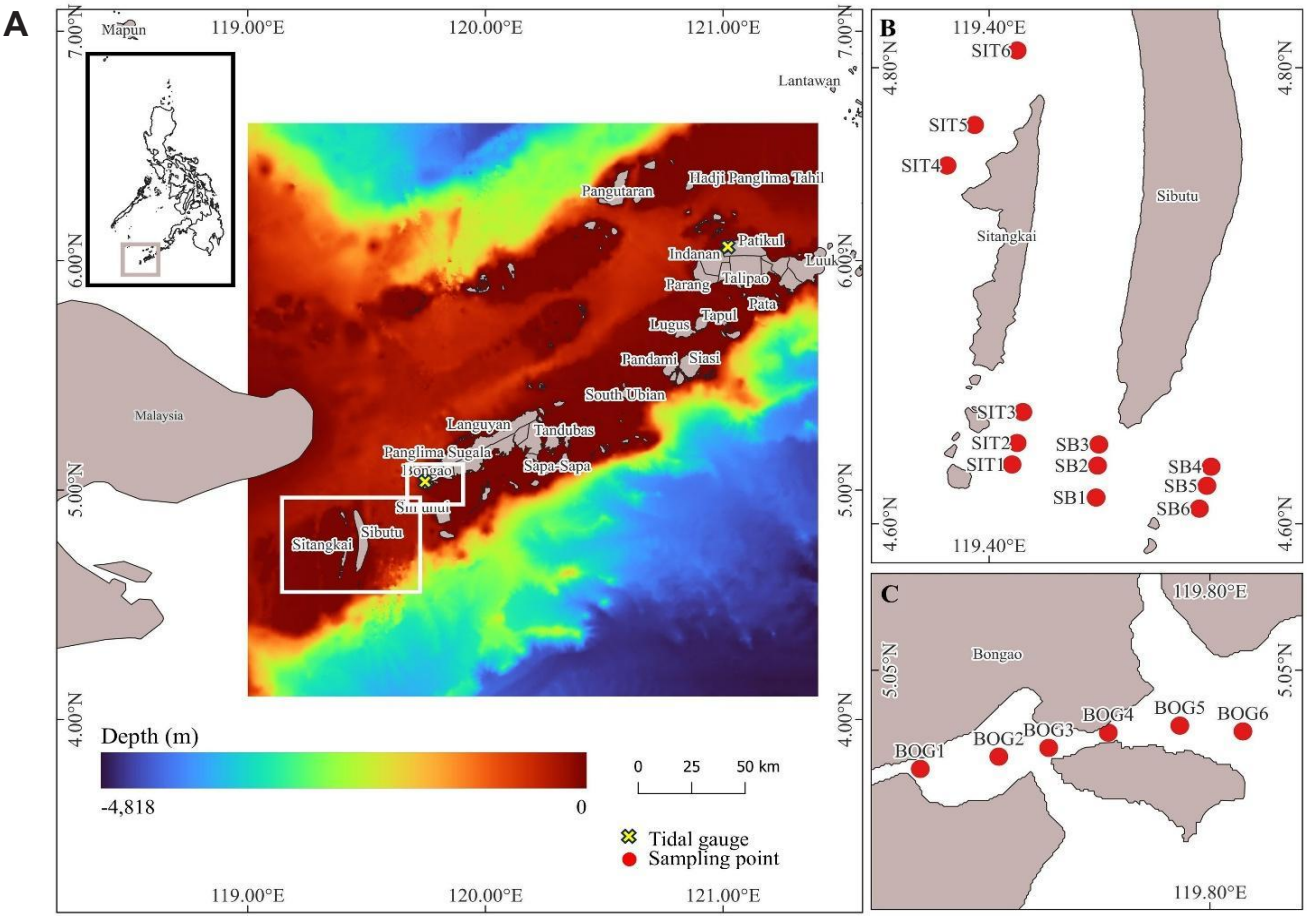

Figure 1. Figure 1. Tawi-Tawi is located in the southernmost part of the Philippines, adjacent to Malaysia. The islands of Sibutu and Sitangkai lie near the border of the country, while Bongao, the capital city, is situated in the southeastern part of Tawi-Tawi (A). Sibutu sampling points (SB1-6) were located in the southern tip of Sibutu Island, while the Sitangkai sampling points (SIT1-6) were distributed in the southeastern and northwestern sides of the island (B). Bongao sampling point (BOG1-6) is situated perpendicular to the coast in the inner waters of Bongao (C). Bathymetry data was extracted from GEBCO Compilation Group (2023): GEBCO 2023 Grid (doi:10.5285/c6612cbe-50b3-0cff-e053-6c86abc09f8f).

Extraction of satellite-derived hydrographic data

Salinity, sea surface temperature (SST), and ocean current velocity fields were derived from the GLOBAL_MULTIYEAR_PHY_001_030:Global Ocean Physics Reanalysis product of the Copernicus Marine Environment Monitoring Service (CMEMS; DOI: 10.48670/moi-00021) with a spatial resolution of 1/12° or ~8 km and a daily temporal resolution. For this study, surface-layer salinity (SSS), potential temperature at the surface (SST), and horizontal current velocity components (eastward *u* and northward *v*) were extracted, from which current speed and direction were computed. The spatio-temporal variability of water current velocity (speed and direction) was examined throughout the monsoon regime, wherein the months of November-March correspond to the northeast monsoon. Further, the months of June-October correspond to the southwest monsoon (Amedo-Repollo et al., 2019). The time frame used was February 26, 2024, to February 25, 2025. An averaged plot of SSS, SST, and water current velocity during February 19-21, 2025, was provided to generate maps within the sampling period. For Chl *a* values, representatives of the sampling month were extracted from Copernicus Marine Service Ocean product OCEANCOLOUR_GLO_BGC_L4_MY_009_104. The product has a daily temporal resolution and 4 km spatial resolution. We used Level-4 (L4) satellite products, which provide daily, gap-filled fields generated through data assimilation and optimal interpolation. In situ sampling dates were therefore matched to the corresponding daily L4 fields, ensuring temporal consistency between field observations and remotely sensed data. Due to the isolated nature of the study site and the lack low-temperature storage, *in situ* Chl *a* measurements were not done. Moreover, SST and SSS were not measured in situ at individual sampling stations; instead, remotely sensed data were used to characterize spatial gradients.

Identification of dominant tidal constituents and variability

Hourly time-series sea level data in Tawi-Tawi (February 2011 - July 2018) and Jolo (January 1984 - December 1995) were acquired from the tide gauge stations of NAMRIA (Geospatial Information Services Division). Missing data were filled with a linear trend and sinusoids from the dominant diurnal (K_1) and semi-diurnal (M_2) constituents of the tide gauges. Inertial oscillations were also added, resulting in a reconstructed sea level dataset (Amedo-Repollo et al., 2021). Using MATLAB R2024b (The Mathworks, Inc., 2024), power spectral density (PSD) plots were used to determine the dominant tidal constituents from each station. PSD distributes the variance of a signal across different frequencies via kinetic energy density peaks (Thomson & Emery, 2014), unveiling a wide range of oceanic motion signals such as tides, inertial oscillations, mesoscale eddies, and El Niño - Southern Oscillation (Chereskin & Roemmich, 1991; Wunsch, 1996).

The dominant tidal constituents from the PSD plots were used to determine each constituent's percent variability using T_Tide, a MATLAB toolbox for time-series tide harmonic analysis (Pawlowicz et al., 2002). Tide constituents were arranged in decreasing amplitude to determine the top constituents with the highest variance (Devlin et al., 2017). Then, the cumulative sum of the top constituents, as well as the 145 available tidal constituents in T_Tide, was calculated using the equation:

$$y_k = \sum_{i=1}^{k} x_i \quad (1)$$

Where y is the total variance (%), x is the constituent-specific tide variance (%), $y_1 = x_1$, $y_2 = x_1 + x_2$, $y_k = y_1 + y_2 \ldots y_k$, with k = 145, the last index of the cumulative summation (Khalafalla et al., 2017). Cumulative sum is an excellent statistical method to reveal any significant incremental increase in the percent contribution of each top tidal constituent with the highest variability among the 145 constituents (Amedo-Repollo et al., 2021). The top constituents (12) accounting to >95% of cumulative sum of tidal variability was plotted along with the hourly sea level at the Tawi-Tawi tide gauge station, to describe tidal current dynamics during the plankton sample collection period (19-21 February 2025).

Virioplankton and picoplankton enumeration and identification

Water samples for virioplankton and picoplankton analyses were collected by pumping water within 1 meter from the surface. Only 2 ml of water from the collected sample was placed in 5-ml cryogenic vials wrapped in aluminum foil and properly labeled. Glutaraldehyde (0.1% final concentration) was used to preserve the samples to allow for longer storage time (Bock et al., 2022). Samples were immediately stored in low temperature in the field, prior to storage in -80°C freezer.

Prior to analysis, samples were thawed at room temperature. Water samples from each station were processed using the CytoFlex S Benchtop Flow Cytometer (Beckman Coulter, USA). Prior to flow cytometric (FCM) enumeration, 1.0 µm fluorescent beads (PolySciences Inc., U.S.) were diluted to a concentration of ~10^5 beads ml^{-1} in filtered seawater, as recommended by epifluorescence microscopy. Partec CyFlow Space (Sysmex) was used to enumerate picophytoplankton (picoeukaryotes, *Synechococcus*, *Prochlorococcus*), viruses, and heterotrophic bacteria (HB). The prepared beads solution was added to the seawater samples for both picophytoplankton and heterotrophic bacteria enumeration at a final concentration of 1% as an FCM internal reference. Since bacteria do not contain any pigments, unlike the autotrophic picophytoplankton, enumeration was made possible by cell DNA staining. The dye SYBR Green I was added to the seawater sample at a final concentration of 10^{-4}, and was allowed to incubate for 10 minutes, prior to cell enumeration. The FCM was calibrated prior to cell enumeration per sampling station.

Carbon biomass (µg C L^{-1}) of the picophytoplankton groups was based on cell abundance, and was estimated by using the average conversion factors of 2590, 255, 36, and 20 fg C $cell^{-1}$ for picoeukaryotes, *Synechococcus*, *Prochlorococcus*, and heterotrophic bacteria, respectively (Buitenhuis et al., 2012; Lee & Fuhrman, 1987). These references provide widely accepted, standardized carbon-to-cell conversion factors for global picoplankton groups in the absence of direct, group-specific size measurements. There are no available conversion factors by biovolume for virioplankton, thus, they are only reported as cell density (cell ml^{-1}). Differences in picoplankton densities for each taxon across the sampling sites were analyzed using One-way Analysis of Variance (ANOVA) followed by pairwise comparisons using the Tukey's HSD test.

RESULTS

Seasonal water current dynamics in the Sulu Archipelago

Monsoonal changes in surface current velocity are more pronounced in the Sulu Sea than in the Celebes Sea and are described here based on seasonal climatologies (Fig. 2). In the Sulu Sea, the northeast monsoon is characterized by a predominantly southward flow originating from the eastern tip of Malaysia and extending toward the Sibutu Passage and the southern waters off Malaysia (Fig. 2A). Current speeds are generally higher during this monsoon regime, with particularly strong southward flow within the Sibutu Passage.

During the southwest monsoon, surface current speeds decrease overall, with the most notable reduction occurring in the Sibutu Passage (Fig. 2B). Changes in current orientation are also evident between monsoon seasons. For example, in the northern waters around Sitangkai and the Sibutu Islands near eastern Malaysia, the southward flow observed during the northeast monsoon shifts to a westward orientation during the southwest monsoon. West of these islands, currents that are predominantly southwestward during the northeast monsoon rotate toward an east–southeast direction during the southwest monsoon. Despite these directional changes, persistent throughflow is maintained within the Sibutu Passage under both monsoon regimes.

In the southern interior of the Sulu Sea, extending eastward from Bongao, surface current speeds are relatively low. In this region, currents are oriented south–southeast during the northeast monsoon and shift toward a south–southwest direction during the southwest monsoon. Farther north, along the Malaysian coast northwest of Bongao (>5.50° N), current direction is predominantly southward during the northeast monsoon, transitioning to a west–southwestward flow during the southwest monsoon.

Quantitative analysis supports these observed patterns. Surface current speed differed significantly between the northeast (Amihan; n = 4,674) and southwest (Habagat; n = 3,895) monsoons (Wilcoxon rank-sum test, W = 10,547,539, $p < 0.001$), with higher mean speeds during Amihan (0.32 ± 0.22 m s^{-1}) than during Habagat (0.26 ± 0.15 m s^{-1}). Differences in current heading between monsoon seasons were also statistically significant when evaluated using vector components. Both the eastward (*u*) and northward (*v*) components differed strongly between Amihan and Habagat (u: W = 10,153,072, $p < 0.001$; v: W = 7,189,247, $p < 0.001$), indicating a significant but relatively small change in current orientation rather than a complete reversal of flow.

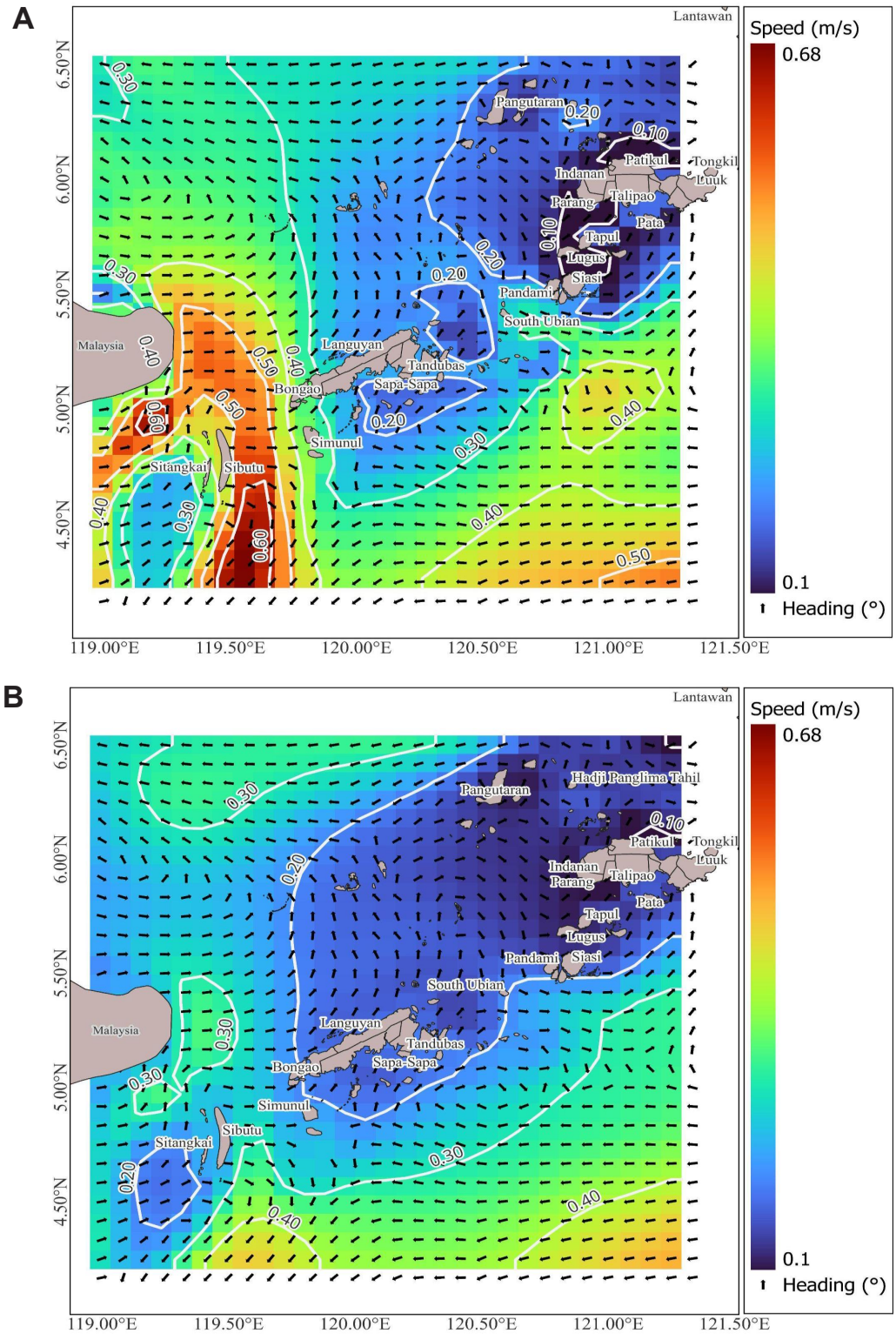

Figure 2. Seasonal climatologies of surface water current velocity (m s^{-1}) during the (A) northeast monsoon (November–March) and (B) southwest monsoon (June–October). Colors indicate current speed and black arrows indicate flow direction. Data were averaged by monsoon season over the period 26 February 2024–25 February 2025 from the Copernicus Marine Service GLOBAL_MULTIYEAR_PHY_001_030 product (DOI: 10.48670/moi-00021)..

Hydrographic profiling in Tawi-Tawi during the sampling period

The temperature and salinity difference between the Sulu Sea (north of the archipelago) and the Celebes Sea (south of the archipelago) revealed the varied properties of water parcels on both sides of the Sulu Archipelago, which potentially mix and enhance nutrient fluxes and productivity (Fig. 3). There is a relatively lower SST observed in the Sulu Sea than in the Celebes Sea (Fig. 3A). The highest values were observed near the coast, while the lowest values were observed in the north of Malaysia at 6.00 °N. In terms of salinity, the lowest value was observed in Malaysia, attributed to tributary rivers from that country (Fig. 3B). Moreover, the highest salinity was observed in the remainder of the Sulu Sea. There are intermediate SSS values observed in the northern Celebes Sea and relatively lower SSS in the southern counterpart.

The water current speed during the sampling period was relatively lower than the current speed during the northeast monsoon regime, with a maximum value of 0.52 m s^{-1} compared to the maximum value of 0.77 m s^{-1} during the entire northeast monsoon regime (Figs. 2A, 4A). The satellite-derived Chl *a* concentration in Tawi-Tawi was observed to be highest around small islands facing the Celebes Sea. Overall, Chl *a* was observed to be concentrated around the small islands of the Sulu Archipelago. A large patch of high Chl *a* can be observed on the southwest side of Sitangkai and Sibutu, a relatively shallow intertidal (Figs. 1A, 4B). Areas away from the archipelago, both in the Sulu and Celebes Seas, had low Chl *a* concentrations.

Dominant tidal constituents and variability in the Sulu Archipelago

At the Tawi-Tawi station, the tide is dominated by the principal semi-diurnal constituents M_2 and S_2 (Fig. 5A), whereas at Jolo, the tide is dominated by the principal diurnal constituents O_1 and K_1 (Fig. 5B). At both stations, the tidal frequency bands carry far more kinetic energy than any other signals in the record – confirming that the observed tides are far more energetic than non-tidal fluctuations.

The tidal constituents collectively explain nearly all of the observed variability at both sites. Tides

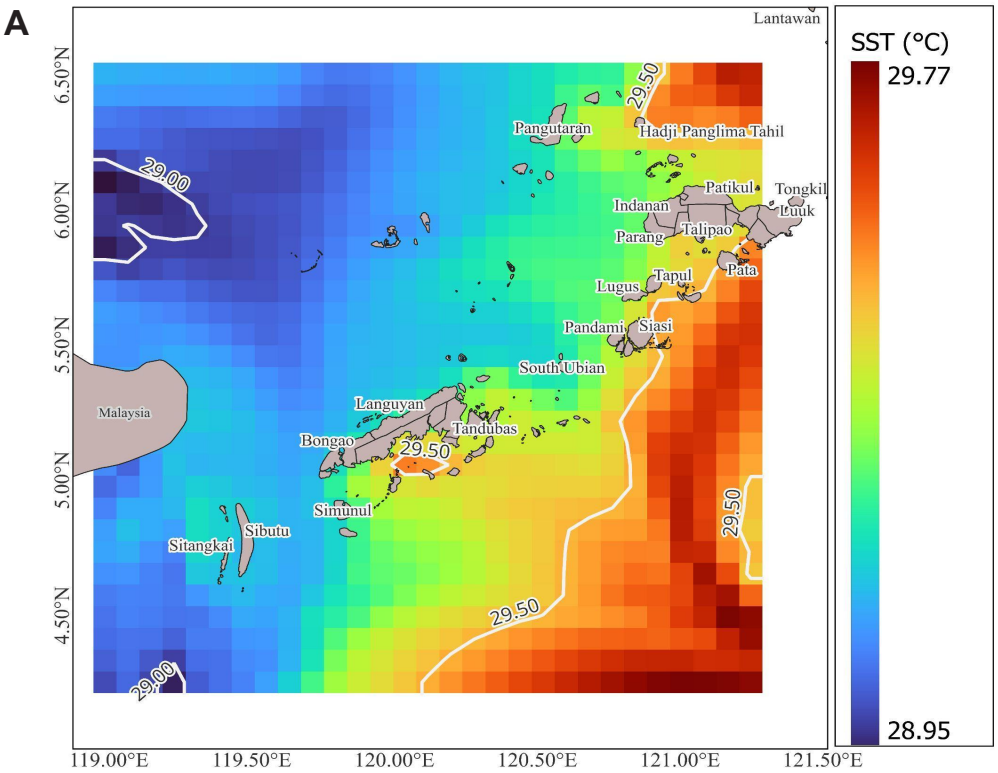

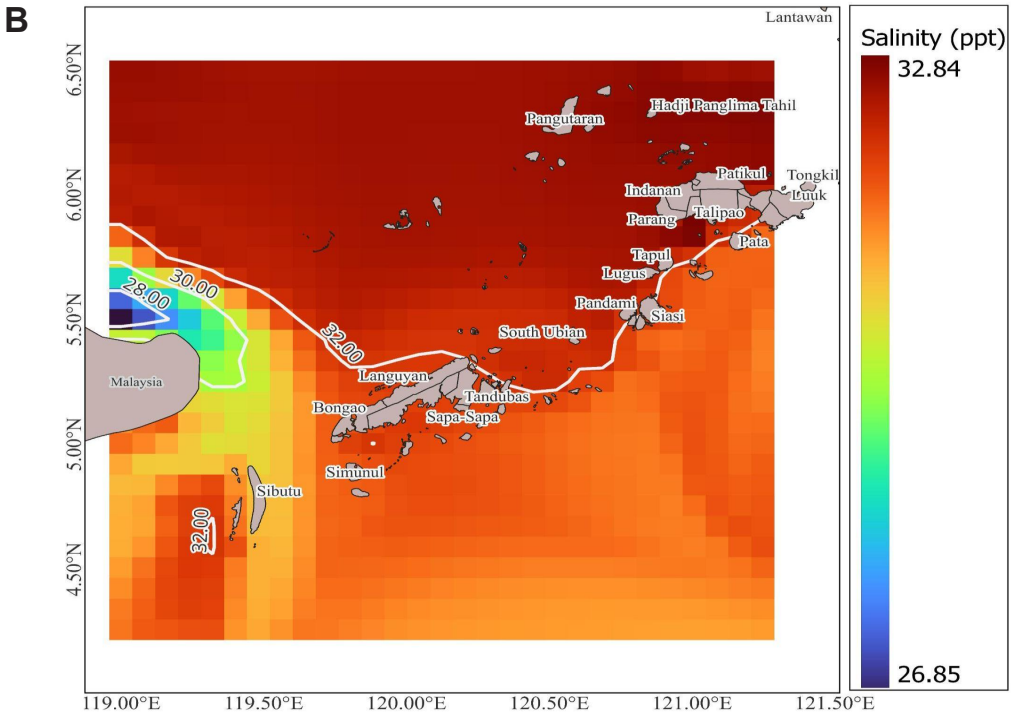

Figure 3. Mean sea surface temperature (A) and salinity (B) profiles in the Sulu Archipelago during the sampling period (19-21 February 2025) extracted from the Copernicus Marine Service GLOBAL_MULTIYEAR_PHY_001_030 product (DOI: 10.48670/moi-00021).

account for about 95.6% of the variance at Tawi-Tawi and 97.3% at Jolo, indicating that tidal forcing is the primary driver of local flow in the Sulu Archipelago (Fig. 6A). Notably, only four constituents – M_2, S_2, K_1, and O_1 – are required to capture the tidal signal at each site, as shown by the sharp rise in cumulative variance once these components are included. This demonstrates that the overwhelming majority of tidal variability is explained by just these principal constituents. These findings reinforce the idea that tidal circulation is the main mechanism for water transport and mixing in the region. Such strong tidal dominance suggests that biological transport processes (e.g., plankton dispersal) will be dominantly influenced by the tidal cycle.

Fig. 6B illustrates the actual sea-level record at the Tawi-Tawi tide gauge station during the plankton sampling period (19-21 February 2025). Note that there was no low tide recorded on 20 February 2025 (Fig. 6B, middle gray rectangle). Despite this missing trough, the key point is that the highlighted sampling window (8:00-11:00) of plankton collection all fall within the period of the highest high water (HHW), that is, the peak of the daily high tide for the whole sampling period.

Density and carbon biomass of picoplankton and femtoplankton (viruses) estimation

The average microbial plankton density in Tawi-Tawi during the sampling period was 2.27×10^6 cells mL^{-1}, comprising both picoplankton and viruses. Sibutu had the highest concentration of microbial plankton at 2.61×10^6 cell mL^{-1}, followed by Bongao with a density of 2.36×10^6 cell mL^{-1}, and Sitangkai with 1.85×10^6 cell mL^{-1} density. Femtoplankton viruses (<0.2 µm) dominated the sample, comprising an average of 78.0% across the three sites, with the highest value recorded in Sitangkai (Fig. 7A). Heterotrophic bacteria accounted for 18.8%, while photosynthetic picoplankton, including picoeukaryotes, *Synechococcus*, and *Prochlorococcus*, were the least abundant at 3.2% (Fig. 7A). Across the three sites, *Synechococcus* was the predominant member of the photosynthetic picoplankton group, accounting for 92.8%, followed by *Prochlorococcus* at 6.5% and picoeukaryotes at 0.7% (Fig. 7B). This distribution highlights the dominance of viral particles and heterotrophic bacteria in the microbial plankton community during the study period.

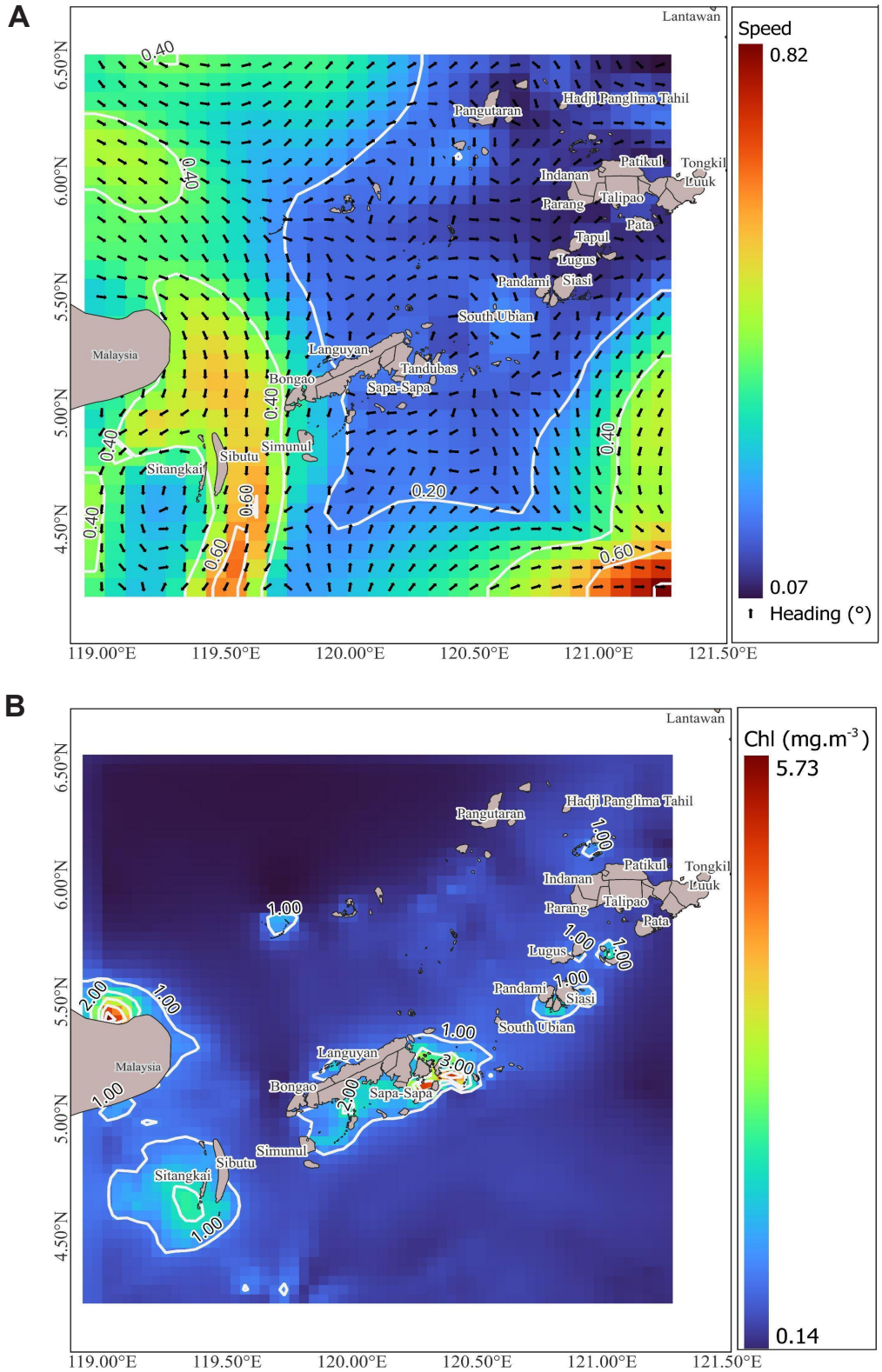

Figure 4. Surface water current velocity (m s-1). Colored gradient represents speed while black arrows represent the direction component of the vector (A). Surface Chl *a* values in the Sulu Archipelago during the sampling period (B; February 19-21, 2025) extracted from the Copernicus Marine Service, OCEANCOLOUR_GLO_BGC_L4_MY_009_104 (DOI: https://doi.org/10.48670/moi-00281) and GLOBAL_MULTIYEAR_PHY_001_030 product (DOI: 10.48670/moi-00021).

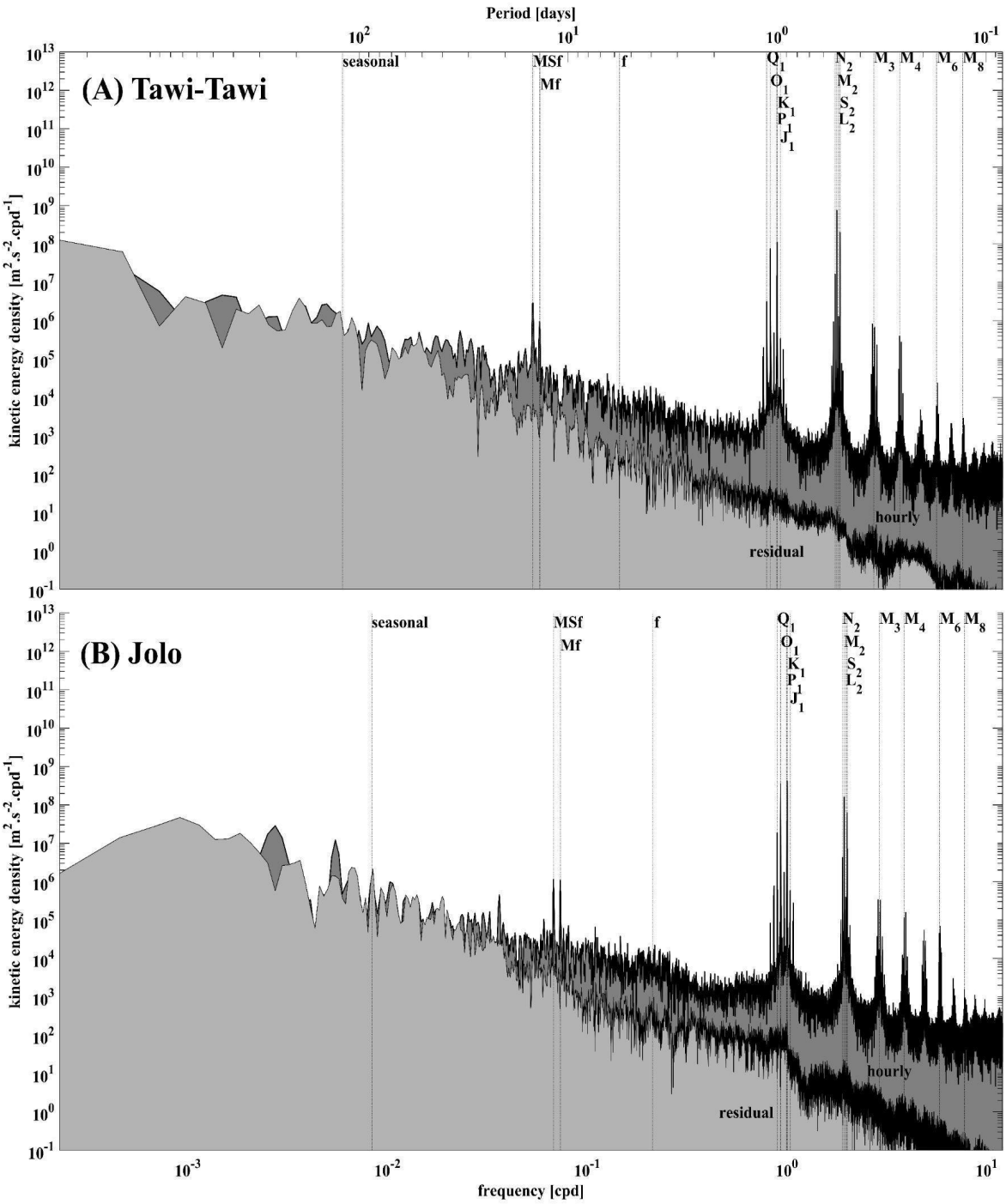

Figure 5. Power spectra of hourly (dark gray) and residual (light gray) tidal sea level in (A) Tawi-Tawi and (B) Jolo tide gauge stations from NAMRIA. The kinetic energy density peaks of diurnal (Q_1, O_1, K_1, P_1, and J_1), semidiurnal (N_2, M_2, S_2, and L_2), overtides (M_3, M_4, M_6, and M_8), long-period tidal constituents (MSf and Mf), inertial oscillation, and seasonal signals are highlighted in the figure.

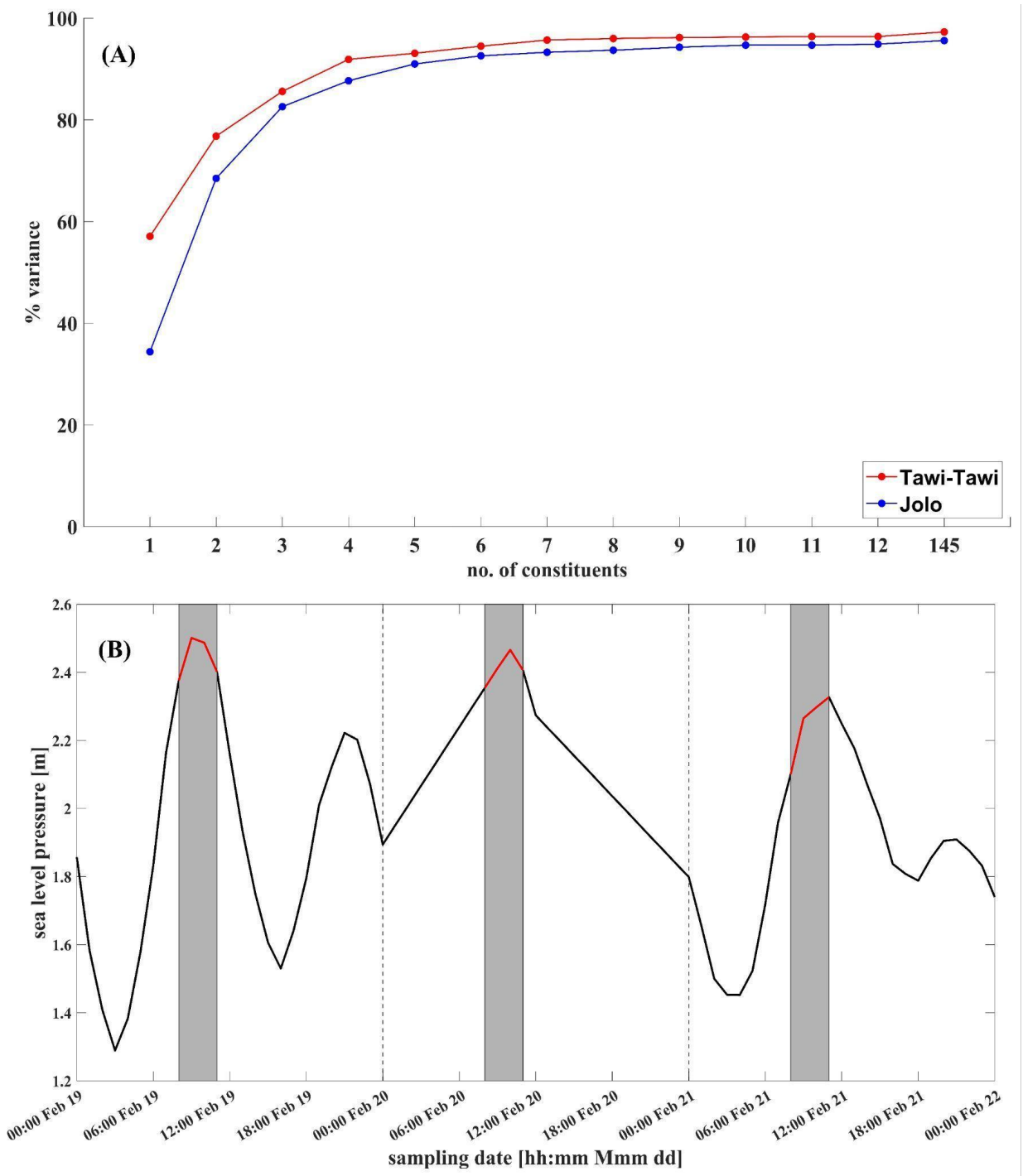

Figure 6. Cumulative summation of increment variance (%) in Tawi-Tawi (red) and Jolo (blue) tide gauge stations (A). For Tawi-Tawi, the first four marked dots are: (a) M_2, (b) M_2 and S_2, (c) M_2, S_2, and K_1. (d) M_2, S_2, K_1. and O_1. For Jolo: (a) K_1, (b) K_1 and O_1, (c) K_1, O_1, and M_2, (d) K_1, O_1, M_2, and S_2. Hourly sea level (m) of the Tawi-Tawi tide gauge station during the sampling period 19-21 February 2025 (B). The actual sampling time (8:00-11:00) is highlighted in (B).

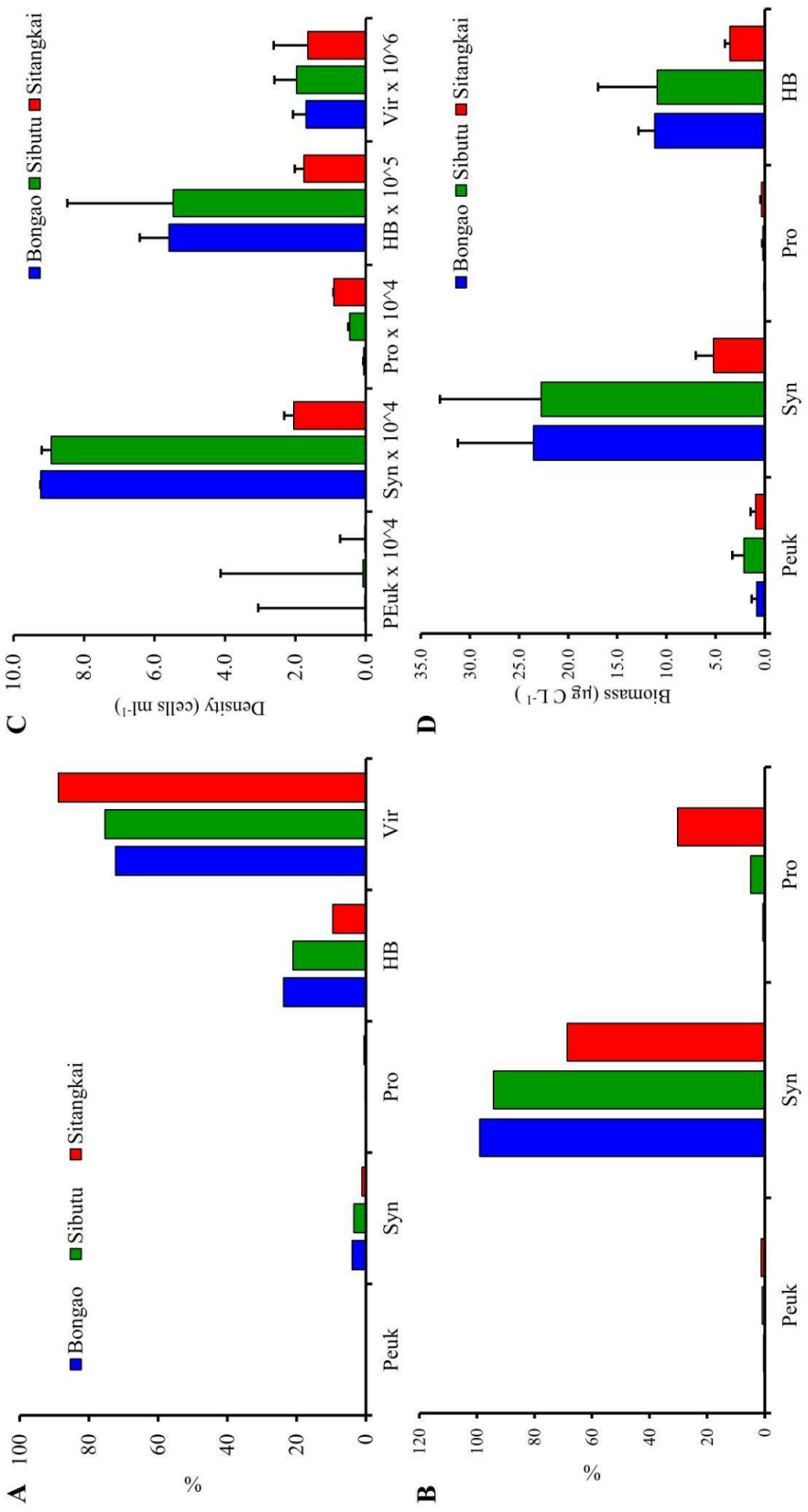

Figure 7. Flow cytometric analysis revealed 5 major groups of picoplankton from Bongao, Sibutu, and Sitangkai. These include Peuk (picoeukaryote), *Synechococcus* (Syn), *Prochlorococcus* (Pro), heterotrophic bacteria (HB), and the femtoplankton viruses (Vir). The overall percent contribution of both picoplankton and femtoplankton (A), and the relative proportions of each autotrophic picoplankton taxon within the group (B) are presented to highlight the dominant taxa and compare among study sites (i.e., color bars). The densities of each group are expressed as cells ml^{-1} (note that each group has different exponents on the x-axis; C). Using published conversion factors, cell densities were converted into biomass (µg C L^{-1}; D). Error bars reflect standard deviation per site. No conversion factors are available for viruses.

Furthermore, Sibutu consistently exhibited high density and biomass of all identified taxa (Supplementary Fig. 1; Fig. 7C, D), likely influenced by the westward tidal currents flowing to the southern region of the island during a flood tide (Figure 8, bottom panels). This is consistent with the observed water level variability from the tide gauge station in Bongao Bay (Figure 6B). Overall, the spatial abundance of microbial plankton in Sibutu is generally higher compared to Sitangkai, as model currents revealed that tidal dynamics in the western sampling sites (Sit 4-6) are dominated by offshore advection during an ebb tide (Figure 8, bottom panels), which potentially account for the reduced abundance.

Subsequently, both Bongao and Sibutu were dominated primarily by *Synechococcus* (Fig. 8A, F), heterotrophic bacteria (Fig. 8D, I), and viruses (Fig. 8E, J). In contrast, *Prochlorococcus* was predominantly abundant in Sibutu and Sitangkai (Fig. 8G), but present at very low concentrations in Bongao (Fig. 8B). The spatial resolution of the model tidal currents (1/12° or 9.2 km × 9.2 km) was too coarse to resolve the dynamics within Bongao Bay (~1.5 km wide). Hence, the general tidal flow could not be inferred from the model, resulting in the lack of current vectors in the plot (Figure 8, top panels). Nevertheless, the variability in this region was mainly driven by differences in proportions among taxa, rather than spatial abundance. Meanwhile, picoeukaryotes, which exhibited the lowest overall concentrations and highest variance, were also more abundant in Sibutu (Fig. 7C).

In detail, femtoplankton viruses had a mean density of 1.8×10^6 cells mL^{-1} and were most abundant in Sibutu, with a density of 2.0×10^6 cells mL^{-1}; however, this difference was not statistically significant compared to the other sites ($p > 0.05$; Fig. 7C). In contrast, heterotrophic bacterial densities in Bongao and Sitangkai were approximately three times higher than those in Sibutu ($p < 0.05$; Fig. 7C). Among autotrophic picoplankton, *Synechococcus* had a mean density of 6.7×10^4 cells mL^{-1} across all stations, but with a significantly lower density recorded in Sitangkai ($p < 0.05$; Fig. 7C). *Prochlorococcus*, with a mean

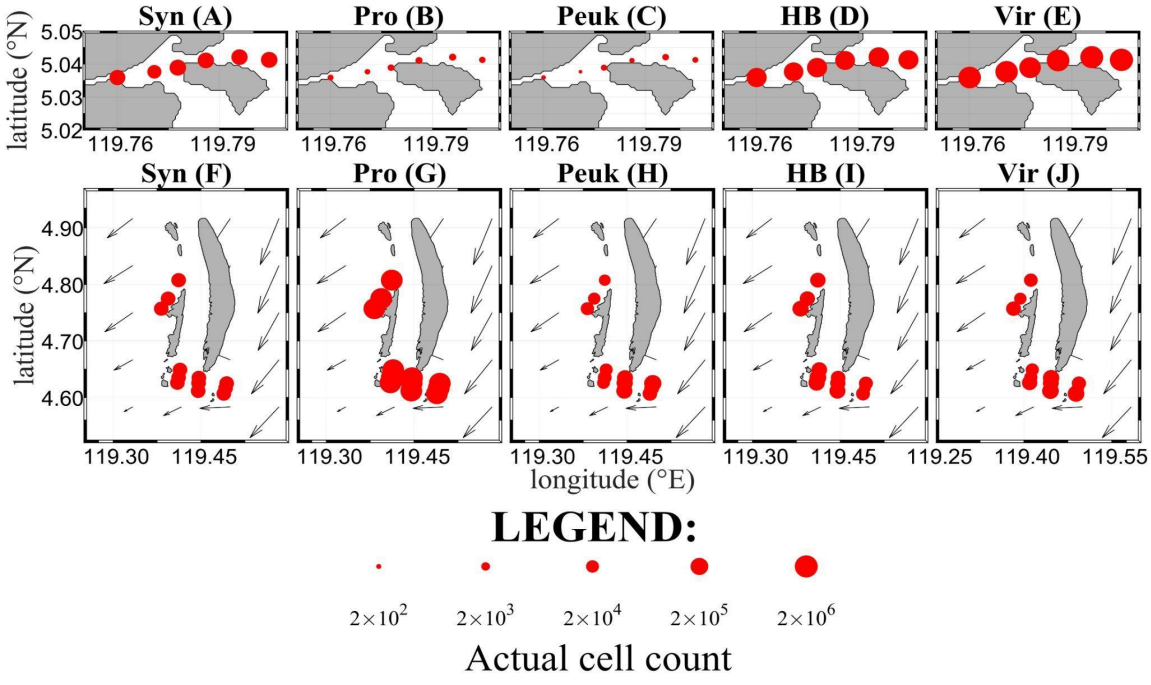

Figure 8. Spatial abundance (log_{10}-transformed) of microbial plankton across Bongao (top panels) and Sibuti-Sitangkai islands (bottom panels). Hourly mean tidal currents during the sampling period (8:00-11:00 AM, 19-21 February 2025) were extracted from Global Ocean Physics Analysis and Forecast dataset (GLOBAL_ANALYSISFORECAST_PHY_001_024, DOI: https://doi.org/10.48670/moi-00016) of Copernicus Marine Service. No tidal currents were plotted near Bongao since the bay's diameter (~1.5 km) is substantially smaller than the product's spatial resolution (1/12° or 9.2 km × 9.2 km).

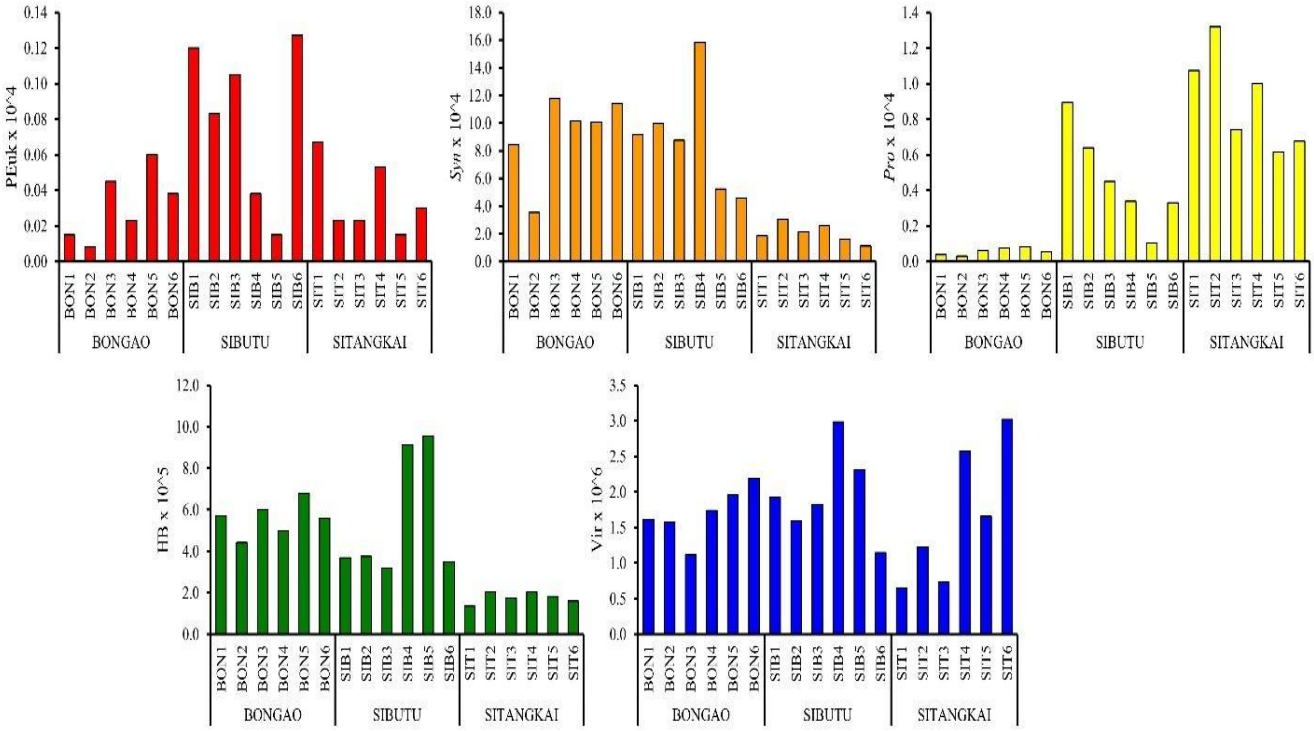

Supplementary Figure 1. Spatial abundance distribution of microbial plankton taxa in Bongao, Sibutu, and Sitangkai.

density of 0.5×10^4 cells mL^{-1}, showed a significant decrease in Bongao, where its concentration was an order of magnitude lower than in the other sites (Fig. 7C). *Prochlorococcus* also exhibited a significant difference when compared between sites (Table 2). Lastly, picoeukaryotes were the least abundant group, with a mean density of 0.05×10^4 cells mL^{-1}, and exhibited a significant increase in Sitangkai, where their density was more than 50% higher than at the other sites (Fig. 7C).

Finally, the estimated mean carbon biomass across all stations was 27.2 µg C L^{-1} (Fig. 7D). Although *Synechococcus* was the second most abundant taxon, it contributed the highest biomass at 17.2 µg C L^{-1}, followed by heterotrophic bacteria with 8.5 µg C L^{-1}, and viruses at 1.7 µg C L^{-1}. *Prochlorococcus* had the lowest biomass contribution (0.17 µg C L^{-1}) among the groups analyzed. It is important to note that the two dominant groups (i.e., *Synechococcus* and heterotrophic bacteria) had low biomass concentrations in Sitangkai (Fig. 7D).

DISCUSSION

Environmental conditions in Tawi-Tawi

Microbial spatial variability across the Sulu Archipelago is closely linked to hydrographic gradients generated by the convergence of contrasting water masses from the Sulu Sea and the Celebes Sea through the Sibutu Passage (Fig. 3). Warmer, fresher waters originating from the Celebes Sea (29.41 °C; 31.52 ppt) and cooler, more saline waters from the Sulu Sea (29.18 °C; 32.31 ppt) create sharp spatial gradients in sea surface temperature and salinity around Bongao, Sibutu, and Sitangkai. The exchange of these water masses across shallow sills and narrow channels promotes strong horizontal advection, while baroclinic tides interacting with complex bathymetry enhance vertical mixing and internal wave activity (Xing and Davies, 2011; Atmadipoera and Suteja, 2018). Together, these processes regulate the redistribution of heat, salt, and nutrients, establishing environmental conditions that act as primary filters shaping spatial patterns in microbial abundance,

structure, and biomass across the archipelago.

Despite these gradients, elevated Chl *a* and plankton biomass, associated with temperature or salinity patterns, suggest that productivity in the region is more strongly linked to current velocity and tidal-driven transport (Fig. 4A–B). Similar current-enhanced chlorophyll signatures have been observed in other parts of the Sulu Sea, such as Panay Gulf during the northeast monsoon (Guirhem-Helican & Acabado, 2024). The hydrography of Tawi-Tawi can therefore affect the picoplankton distribution across the Sulu Archipelago. Further, the shallow shelves (<200 m) fringing Bongao, Sibutu, and Sitangkai create localized retention zones where tidal currents are slow, allowing plankton aggregation and enhancing nutrient residence times (Almroth-Rosell et al., 2016; Odebrecht et al., 2015). Further, the shallow bathymetry (<200 m) around Bongao, Sibutu, and Sitangkai exemplified the dynamic environment in which the Sulu Sea and Celebes Sea interact. The shallow bathymetry areas can provide more localized retention zones that can enhance plankton growth due to enhanced mixing around the area (Almroth-Rosell et al., 2016; Odebrecht et al., 2015).

Monsoonal and tidal currents as drivers of transport

Building on the contrasting hydrographic background set by the Sulu and Celebes Seas, it is the tidal and monsoonal currents that are likely to determine how these water masses interact and how nutrients and plankton are redistributed across the archipelago. The water currents driving horizontal advection in the Sulu Archipelago are predominantly forced by tides, as confirmed by the results of this study. The spectral analysis revealed that tidal constituents accounted for the highest peaks in the kinetic energy density (Fig. 5). The cumulative variance explained by tides reached 95.6% (M_2 = 57.1%, S_2 = 19.7%, K_1 = 8.3%, O_1 = 6.3%) at Tawi-Tawi and 97.3% (K_1 = 34.4%, O_1 = 34.1%, M_2 = 14.1%, S_2 = 5.1%) at Jolo (Fig. 6A), consistent with Ajoc et al. (2025, *unpubl. data*), who similarly found spectral peaks of the same tide gauge stations. These results confirm that tidal currents are the primary drivers of variability and transport in the region. Furthermore, hourly sea level records from the Tawi-Tawi tide gauge during the sampling period (19-21 February 2025) indicate that plankton samples were collected during the HHW (Fig. 6B), coinciding with peak tidal amplitudes. It should be noted that on the 20th of February 2025, the Tawi-Tawi station did not record a low tide, despite semi-diurnal tides being observed in the preceding and succeeding days of the sampling period (Fig. 6B). This absence likely reflects a data gap or instrument anomaly at the gauge rather than a physical tidal event (Pugh & Woodworth, 2014). Nevertheless, this brief malfunction does not alter the broader consensus that tidal forcing dominates the observed variability in the region.

In connection with this, there is a relatively lower water current speed during the study period than the broader northeast monsoon regime (maximum 0.52 m s^{-1} vs. 0.77 m s^{-1}). This water current speed, however, is not as weak as that generally observed during the southwest monsoon (Fig. 2B). Field and modeling studies show that frontal and plume-driven currents on the order of ~0.3–0.4 m s^{-1} can concentrate and rapidly transport plankton across shelves and fronts, substantially altering their horizontal and vertical distributions (Scotti et al., 2007; Peterson et al., 2009), supporting the role of current-driven accumulation and mixing in shaping planktonic and microbial patterns. This suggests that localized retention processes through the Sibutu Channel between the Sulu and Celebes Seas were the driving forces for enhanced natural productivity in these areas (Almroth-Rosell et al., 2016; Odebrecht et al., 2015). In contrast, the Bongao stations showed weaker Chl *a* signals, consistent with relatively lower current-driven fluxes east of the island.

Horizontal physical transport and vertical nutrient flux in the Sulu Archipelago

The dominance of semi-diurnal tidal constituents (M_2 and S_2) at the Tawi-Tawi tide gauge station indicates frequent oscillations of flood and ebb currents near the sampling sites of Bongao, Sitangkai, and Sibutu Islands. Tidal ellipses of M_2 currents in the Sulu Archipelago reveal consistently strong tidal flows oriented along the north-south axis parallel to southern Sitangkai and Sibutu Islands (Jing et al., 2012). The proximity of the sampling sites to this dynamic region likely enhances plankton retention near the coast through tidal current-induced horizontal advection (Blauw et al., 2012).

Baroclinic tides play a crucial role in vertical nutrient fluxes in the Sulu Archipelago, where the interaction of barotropic tides from the Celebes Sea with steep bathymetry south of the region generates internal tides (Jing et al., 2012), reaching depths >1000 meters (Girton et al., 2011). Internal tides enhance vertical mixing and bring nutrient-rich deep

waters into the euphotic zone through persistent upwelling (Rogers et al., 2022), stimulating primary productivity as evidenced by elevated satellite-derived Chl *a* near the southern coast compared to the north (Fig. 4B). Enhanced surface-layer picoplankton and virioplankton biomass at sampling stations south of Sitangkai, Sibutu, and Bongao further support this nutrient enrichment from tidal dynamics (Fig. 8). Additionally, plankton sampling during HHW aligns with stronger vertical mixing and upwelling, which together enhance nutrient flux, redistribute plankton in the upper water column, and increase horizontal advection toward sampling sites via tidal currents (Sharples et al., 2001; Rogers et al., 2022; Nash et al., 2006; Blauw et al., 2012). These synergistic processes likely contribute to the elevated plankton biomass observed during sampling.

Pico- and femtoplankton in Tawi-Tawi

The microbial plankton community in the Sulu Archipelago, particularly around Tawi-Tawi, exhibited a distinct structure during the study period, characterized by the dominance of femtoplankton viruses and heterotrophic bacteria. The *in-situ* data were observed to match the Chl *a* concentration from satellite data, such as higher total microbial density in Sibutu compared to Sitangkai (Figs. 4B, 7). The average microbial density was 2.27×10^{6} cells mL^{-1}, with viruses accounting for the majority (78%) of this population, consistent with findings in other tropical marine systems where viral particles outnumber cellular plankton groups (Suttle, 2007). In terms of carbon biomass, *Synechococcus* contributed the highest biomass despite not being the most numerically dominant group, underscoring

Table 1. Correlation analysis of picoplankton and femtoplankton groups in Tawi-Tawi Islands

	Picoeukaryote	*Synechococcus*	*Prochlorococcus*	Heterotrophic Bacteria	Viruses
Picoeukaryote	1.00				
Synechococcus	0.19	1.00			
Prochlorococcus	0.22	-0.53	1.00		
Heterotrophic Bacteria	-0.18	**0.71**	**-0.71**	1.00	
Viruses	-0.13	0.27	-0.17	0.39	1.00

Table 2. Pairwise-comparisons between islands using Tukey's HSD test following significant results from One-way ANOVA. Bog-Sib = Bongao vs. Sibutu, Bog-Sit = Bongao vs. Sitangkai, and Sib-Sit = Sibutu vs. Sitangkai. Bold p values indicate significant differences

Pairwise - comparison	Peuk	Syn	Pro	HB	Vir
Bog-Sib	$p > 0.05$	$\mathbf{p < 0.05}$	$\mathbf{p < 0.05}$	$\mathbf{p < 0.05}$	$p > 0.05$
Bog-Sit	$\mathbf{p < 0.05}$	$p > 0.05$	$\mathbf{p < 0.05}$	$p > 0.05$	$p > 0.05$
Sib-Sit	$p > 0.05$	$\mathbf{p < 0.05}$	$\mathbf{p < 0.05}$	$\mathbf{p < 0.05}$	$p > 0.05$

its ecological importance as a primary producer in these coastal waters. Heterotrophic bacteria followed as a substantial carbon sink, reflecting their role in carbon remineralization. The notably lower biomass of *Prochlorococcus* is typical of its smaller cell size compared to *Synechococcus*, in addition to its low density in Tawi-Tawi (Scanlan et al., 2009).

Heterotrophic bacterial density was significantly higher in Bongao and Sitangkai compared to Sibutu, matter (i.e., viral shunt; Fuhrman, 1999). Therefore, viruses play a role in regulating the abundance of heterotrophic bacteria in this study, allowing also the continuous supply of nutrients for new bacterial growth.

In addition, among the autotrophic picoplankton, *Synechococcus* was the most abundant taxon (92.8% of photosynthetic picoplankton), followed by *Prochlorococcus* and picoeukaryotes (Fig. 7B). This

Table 3. Picoplankton biomass comparison with tropical and subtropical data

Group	Tawi-Tawi (this study)	Kuroshio Seamount (Acabado and Chen, unpubl.)	Batan Bay Estuary (Sibulan and Acabado, unpubl.)	Gulf of Mexico (Linacre et al., 2015)
	Mean Biomass (µg C L^{-1})			
Picoeukaryote	1.28	4.7	5	3.10
Synechococcus	**17.17**	**7.0**	**28.6**	1.70
Prochlorococcus	0.17	0.5	4.6	8.58
Heterotrophic bacteria	8.54	1.3	-	11.22

suggesting that localized environmental factors such as organic matter inputs or retention zones might enhance bacterial growth in these areas (Table 2; Fig. 7C). Conversely, femtoplankton viral densities were fairly consistent across sites, indicating a ubiquitous viral presence likely linked to host availability (Table 2; Fig. 7C). The predominance of viruses in the plankton community highlights the significant role of viral lysis in nutrient cycling and microbial mortality, particularly affecting heterotrophic bacteria within the Sulu Archipelago's planktonic food webs. Viral lysis is a key step in biogeochemical cycling in the oceans (Shelford et al., 2012; Wilhelm & Suttle, 1999). This result is further supported by the observed positive, though weak, correlation between viral and bacterial densities, indicating a dynamic interaction where viruses regulate bacterial populations while contributing to nutrient recycling (Table 1). This bacterial host-virus dynamics may be explained in the context of the microbial loop, where viruses are obligate parasites that kill their host by lysis. However, lysis of bacterial cells releases labile contents of the cells, which allows the continuous cycling of organic

aligns with previous observations in oligotrophic to mesotrophic tropical seas, where *Synechococcus* frequently dominates the cyanobacterial community due to its ubiquitous distribution and adaptability to a wide range of nutrient conditions (Scanlan et al., 2009; Flombaum et al., 2013). This pattern of *Synechococcus* dominance was also observed in the productive Batan Bay Estuary, Aklan, and an oligotrophic seamount in the Kuroshio, highlighting the wide range of nutrient concentration tolerance of the taxon (Table 3; Acabado et al., *unpubl. data*; Sibulan & Acabado, *unpubl. data*). The lower abundance of *Prochlorococcus* in Bongao compared to Sibutu and Sitangkai may reflect spatial variability in nutrient availability or hydrodynamic conditions influencing water mass characteristics, considering the semi-enclosed topography in Bongao (Partensky et al., 1999).

The observed spatial heterogeneity in plankton distribution and biomass in the Sulu Archipelago likely results from a combination of physical, chemical, and biological factors. Although diel vertical migration (DVM) is often considered a dominant process

among planktonic groups, DVM is unlikely to affect the observed patterns in Tawi-Tawi. The intensity and amplitude of DV are strongly cell size-dependent, where smaller cells like picoplankton exhibit reduced vertical capacity for migration compared to larger zooplankton (Hays et al., 2001). In addition, and more critically, Tawi-Tawi is subjected to significant physical forcing (i.e., tides and currents) which can likely prevent coherent DVM structuring in the coastal waters (Kamykowski, 1995).

Hydrodynamic features such as water currents, tides, and retention zones influence plankton transport and aggregation (Yu et al., 2019). The intermediate flow in Tawi-Tawi (0.52 m s^{-1}) may favor plankton accumulation around shallow island shelves by reducing advective losses without completely limiting nutrient exchange area, as was observed southwest of Sitangkai and Sibutu Passage with elevated Chl *a* (Fig. 4A; Almroth-Rosell et al., 2016; Ferrera et al., 2018; Odebrecht et al., 2015). Enhanced picoplankton and virioplankton biomass south of Sitangkai, Sibutu, and Bongao reflects nutrient enrichment driven by strong tidal mixing and upwelling during HHW, which promotes vertical nutrient flux, redistributes plankton in the upper water column, and intensifies horizontal advection via tidal currents toward sampling sites, collectively elevating plankton biomass in the Sulu Archipelago (Figs. 6B, 7) during daytime HHW under a neap tide phase.

Picoplankton productivity is generally pronounced during daytime and obscured at night, whereas virioplankton showed no clear diel pattern (Chen et al., 2021). Higher pico- and virioplankton abundances are typically observed during the spring compared to neap tide (Chen et al., 2019; Sharples et al., 2007), while flood tides generally showed more evident abundance in contrast to ebb tides (Xie et al., 2024). In this study, the sampling period was conducted during a post-flood current at HHW, which could likely be the highest pico- and virioplankton abundance under a neap tide. However, abundance is possibly the highest if samples were collected during a spring tide at night.

Nevertheless, the observed dominance of viruses and heterotrophic bacteria likely reflects their ability to thrive in nutrient-enriched retention zones where organic matter accumulates, while the prevalence of *Synechococcus* indicates its adaptability to dynamic mixing conditions that continually resupply nutrients to the euphotic layer (Samo et al., 2012; Schimdt et al., 2020). These findings underscore the importance of integrating microbial dynamics and hydrographic context to better understand coastal ecosystem functioning in archipelagic environments.

CONCLUSIONS

This study investigated a snapshot spatial distribution and abundance of microbial plankton in Tawi-Tawi during daytime HHW of a neap-tide regime. The hydrographic environment around Tawi-Tawi and the Sulu Archipelago is defined by a complex interaction of distinct water masses from the cooler, saltier Sulu Sea in the north and the warmer, less saline Celebes Sea in the south, which together generate strong spatial gradients in sea surface temperature and salinity. These gradients, however, do not directly correlate with patterns of biological productivity as indicated by Chl *a* and plankton biomass, suggesting that physical transport and retention processes exert a stronger influence on ecosystem dynamics than hydrographic gradients alone. Slow to intermediate current velocities observed in the region, combined with strong tidal forcing in shallow bathymetric areas (i.e., Sibutu and Sitangkai), create retention zones that enhance both horizontal advection and vertical nutrient fluxes, thereby sustaining high picoplankton productivity.

The prevalence of semidiurnal and diurnal tidal signal variability (>95%) from our PSD and variance plots proves that tides are the main drivers of horizontal advection and vertical mixing in the region. Moreover, the interplay of hydrography characterized by slow currents and tidal mixing, along with the adaptive biological traits of picoplankton and viruses, determines the spatial variability in nutrient concentration, plankton abundance, and productivity within the Sulu Archipelago. This integrative perspective is key to understanding ecosystem functioning and resilience in archipelagic marine environments subject to both natural variability and increasing anthropogenic pressures.

The predominance of semi-diurnal tidal variability and associated internal baroclinic tides generated by bathymetric interactions in the Tawi-Tawi Islands further drives horizontal advection, vertical mixing, and upwelling of deep nutrient-rich waters into the euphotic zone. This enrichment is reflected in the elevated picoplankton and virioplankton biomass observed at the southern sampling stations of Sitangkai, Sibutu, and Bongao, where the coupling

of horizontal advection with vertical fluxes during tidal phases (notably HHW) facilitated redistribution and accumulation of microbial plankton. Such physical-biological interactions help explain how the region sustains productivity despite the oligotrophic nature of the surrounding seas.

Biological tolerances also shape microbial community structure. The dominance of femtoplankton viruses and heterotrophic bacteria reflects viral control over bacterial populations through lysis, influencing nutrient regeneration and microbial mortality rates that underpin food web dynamics. Similar to other regions, *Synechococcus* emerges as the leading autotrophic picoplankton in Tawi-Tawi due to its ecological adaptability and capacity to thrive across varying nutrient conditions, in contrast to the spatially patchy distribution of *Prochlorococcus* and generally lower abundance of picoeukaryotes. These biological traits, combined with the physical oceanographic context, regulate the distributional heterogeneity of plankton communities.

In summary, the interplay of hydrography characterized by slow currents and tidal mixing, along with the adaptive biological traits of picoplankton and viruses, determines the spatial variability in nutrient concentration, plankton abundance, and productivity within the Sulu Archipelago. This integrative perspective is key to understanding ecosystem functioning and resilience in archipelagic marine environments subject to both natural variability and increasing anthropogenic pressures.

However, the one-time sampling nature of plankton data limits the ability to fully capture temporal variability in productivity and physical transport processes in the region. Future work should prioritize long-term monitoring of plankton communities, nutrient, and biogeochemical cycles to better resolve seasonal and interannual dynamics. Despite these limitations, the combination of spectral density and cumulative variance of tides from extensive *in situ* sea level data, supported by historical observations, provides robust evidence that tidal forcing reinforces both the transport and productivity of picoplankton and virioplankton in the southwestern islands of the Sulu Archipelago.

ACKNOWLEDGEMENTS

The authors thank Dr. Tzong-Yueh Chen of the Institute of Marine Environment and Ecology, National Taiwan Ocean University, for assistance with picoplankton analyses. Gratitude is also extended to the OVCRIDE research staff of MSU-TCTO (Mohammad Amilussin Ammang, Alimar Sakilan, and Akkil Injani) and the PlanktoNiche Laboratory project personnel and student assistants (Severino Agliam III, Josave D. Oczon, and Carl Bryle Rosal) for their support. The authors also thank Mr. Shelmark Peñaranda of the Physical Oceanography Division and the Geospatial Information Services Division of NAMRIA for providing multi-year sea level data from tide gauge stations in Tawi-Tawi and Jolo. This study was made possible through the funding from the DOST-PCAARRD-GIA research grant as an offshoot output from the *Pinctada* Project.

ETHICAL DECLARATION

The authors declare that no human participants or animals were involved in this research, and therefore, ethical approval was not required.

CONFLICT OF INTEREST STATEMENT

The author(s) declared that this work was conducted in the absence of any commercial or financial relationships that could be construed as a potential conflict of interest.

LITERATURE CITED

Acabado, C.S., C-C. Chen, M-H. Chang. Effects of the flow-seamount interaction and Kelvin-Helmholtz billow-induced upward nitrate flux on picoplankton communities along the Kuroshio. [Unpublished PhD dissertation]. National Taiwan Normal University

Ajoc, S. M., Amedo-Repollo, C. L., & Villanoy, C. L. (2025). Investigating the influence of tides on water column productivity in the Sulu Ridge, Philippines. [Unpublished master's thesis]. Marine Science Institute

Almroth-Rosell, E., Edman, M., Eilola, K., Meier, H. E. M., & Sahlberg, J. (2016). Modelling nutrient retention in the coastal zone of a eutrophic sea. Biogeosciences, 13(20), 5753–5769.https://doi.org/10.5194/bg-13-5753-2016

Amedo-Repollo, C. L., Flores-Vidal, X., Chavanne, C., Villanoy, C. L., & Flament, P. (2021). Barotropic and baroclinic tides in Panay Strait, Philippines. *Regional Studies in Marine Science*, 41, 101612. https://doi.org/10.1016/j.rsma.2021.101612

Atmadipoera, A. S., & Suteja, Y. (2018). Deep water masses exchange induced by internal tidal waves in Ombai Strait. *IOP Conference Series Earth and Environmental Science*, 176, 012017. https://doi.org/10.1088/1755-1315/176/1/012017

Baker, B. B. (2007). Tidal analysis and prediction. In *NOAA Special Publication NOS CO-OPS 3* (No. 2007925298). National Oceanic and Atmospheric Administration. Retrieved September 14, 2025, from https://tidesandcurrents.noaa.gov/publications/Tidal_Analysis_and_Predictions.pdf

Blauw, A. N., Benincà, E., Laane, R. W. P. M., Greenwood, N., & Huisman, J. (2012). Dancing with the Tides: Fluctuations of Coastal Phytoplankton Orchestrated by Different Oscillatory Modes of the Tidal Cycle. *PLoS ONE*, 7(11), e49319. https://doi.org/10.1371/journal.pone.0049319

Bock, N., Subramaniam, A., Juhl, A. R., Montoya, J., & Duhamel, S. (2022). Quantifying Per-Cell Chlorophyll a in Natural Picophytoplankton Populations Using Fluorescence-Activated Cell Sorting. *Frontiers in Marine Science*, 9. doi:10.3389/fmars.2022.850646

Bouman, H. A., Ulloa, O., Barlow, R., Li, W. K. W., Platt, T., Zwirglmaier, K., Scanlan, D. J., & Sathyendranath, S. (2011). Water-column stratification governs the community structure of subtropical marine picophytoplankton. *Environmental Microbiology Reports*, 3(4), 473–482. https://doi.org/10.1111/j.1758-2229.2011.00241.x

Chen, X., Wei, W., Wang, J., Li, H., Sun, J., Ma, R., Jiao, N., & Zhang, R. (2019). Tide driven microbial dynamics through virus-host interactions in the estuarine ecosystem. *Water Research*, 160, 118–129. https://doi.org/10.1016/j.watres.2019.05.051

Chen, T., Lai, C., Tai, J., Ko, C., & Shiah, F. (2021). Diel to seasonal variation of picoplankton in the tropical South China Sea. *Frontiers in Marine Science*, 8. https://doi.org/10.3389/fmars.2021.732017

Chereskin, T.K. & Roemmich, D. (1991). A Comparison of Measured and Wind-derived Ekman Transport at 11°N in the Atlantic Ocean. *Journal of Physical Oceanography*, 21(6), 869-878.

Chisholm, S. W. (1992). Phytoplankton Size. In P. G. Falkowski, Woodhead, A.D., Vivirito, K. (Ed.), Primary Productivity and Biogeochemical Cycles in the Sea. Environmental Science Research (Vol. 43). Boston, MA.: Springer.

Chu, P. C., Liu, Q., Jia, Y., & Fan, C. (2002). Evidence of a Barrier Layer in the Sulu and Celebes Seas. *Journal of Physical Oceanography*, 32, 3299–3309. doi:10.1175/1520-0485(2002)032<3299:EOABLI>2.0.CO;2

Collado-Fabbri, S., Vaulot, D., & Ulloa, O. (2011). Structure and seasonal dynamics of the eukaryotic picophytoplankton community in a wind-driven coastal upwelling ecosystem. *Limnology and Oceanography*, 56(6), 2334–2346. https://doi.org/10.4319/lo.2011.56.6.2334

De Falco, C., Desbiolles, F., Bracco, A., & Pasquero, C. (2022). Island Mass Effect: A Review of Oceanic Physical Processes. Frontiers in Marine Science, 9. doi:10.3389/fmars.2022.894860

Devlin, A. T., Jay, D. A., Zaron, E. D., Talke, S. A., Pan, J., & Lin, H. (2017). Tidal variability related to sea level variability in the Pacific Ocean. *Journal of Geophysical Research Oceans*, 122(11), 8445–8463. https://doi.org/10.1002/2017jc013165

Ferrera, C. M., Jacinto, G. S., Chen, C.-T. A., & Lui, H.-K. (2018). Organic Carbon Concentrations in High- and Low-Productivity Areas of the Sulu Sea. *Sustainability*, 10(6), 1867. https://doi.org/10.3390/su10061867

Flombaum, P., Gallegos, J. L., Gordillo, R. A., Rincón, J., Zabala, L. L., Jiao, N., . . . Martiny, A. C. (2013). Present and future global distributions of the marine Cyanobacteria Prochlorococcus and *Synechococcus*. *Proceedings of the National Academy of Sciences*, 110(24), 9824-9829. doi:10.1073/pnas.1307701110

Fuhrman, J. A. (1999). Marine viruses and their biogeochemical and ecological effects. *Nature*, 399(6736), 541–548. https://doi.org/10.1038/21119

Girton, J., Chinn, B., & Alford, M. (n.d.). Internal Wave Climates of the Philippine Seas. *Oceanography*, 24(01), 100–111. https://doi.org/10.5670/oceanog.2011.07

Gordon, A. L., Huber, B. A., Metzger, E. J., Susanto, R. D., Hurlburt, H. E., & Adi, T. R. (2012). South China Sea throughflow impact on the Indonesian throughflow. *Geophysical Research Letters*, 39(11). doi:10.1029/2012gl052021

Grob, C., Ulloa, O., Claustre, H., Huot, Y., Alarcon, G., & Marie, D. (2007). Contribution of picoplankton to the total particulate organic carbon concentration in the eastern South Pacific. *Biogeosciences*, 4, 837-852. doi:hal-00330328

Guirhem-Helican, G. L., & Acabado, C. S. (2024). Chlorophyll-a interannual and seasonal variability in Panay Gulf: Identification of potential productive sites in the municipal waters and offshore blooms aided by water currents. *Regional Studies in Marine Science*, 80, 103881. https://doi.org/10.1016/j.rsma.2024.103881

Hays, G. C., Harris, R. P., & Head, R. N. (2001). Diel changes in the near-surface biomass of zooplankton and the carbon content of vertical migrants. *Deep-Sea Research* II, 48, 1063-1068. https://doi.org/10.1016/S0967-0645(00)00109-0

Jackson, C. R., Arvelyna, Y., & Asanuma, I. (2011). High-frequency nonlinear internal waves around the Philippines. *Philippine Straits Dynamics Experiment*, 24(1), 90–99. https://www.jstor.org/stable/24861242

Jiao, N., Yang, Y., Hong, N., Ma, Y., Harada, S., Koshikawa, H., & Watanabe, M. (2005). Dynamics of autotrophic picoplankton and heterotrophic bacteria in the East China Sea. *Continental Shelf Research*, 25(10), 1265-1279. doi:10.1016/j.csr.2005.01.002

Jing, Z., Qi, Y., & Du, Y. (2012). Persistent upwelling and front over the Sulu Ridge and their variations. *Journal of Geophysical Research Atmospheres*, 117(C11). https://doi.org/10.1029/2012jc008355

Kamykowski, D. (1995). TRAJECTORIES OF AUTOTROPHIC MARINE DINOFLAGELLATES. *Journal of Phycology*, 31(2), 200–208. https://doi.org/10.1111/j.0022-3646.1995.00200.x

Kossack, J., Mathis, M., Daewel, U., Zhang, Y. J., & Schrum, C. (2023). Barotropic and baroclinic tides increase primary production on the Northwest European Shelf. *Frontiers in Marine Science*, 10. https://doi.org/10.3389/fmars.2023.1206062

Li, J., Liu, X., Xie, N., Bai, M., Liu, L., Sen, B., & Wang, G. (2023). Subsurface Bacterioplankton Structure and Diversity in the Strongly-Stratified Water Columns within the Equatorial Eastern Indian Ocean. *Microorganisms*, 11(3), 592. https://doi.org/10.3390/microorganisms11030592

Marie, D., Partensky, F., Jacquet, S., & Vaulot, D. (1997). Enumeration and Cell Cycle Analysis of Natural Populations of Marine Picoplankton by Flow Cytometry Using the Nucleic Acid Stain SYBR Green I. *Applied and Environmental Microbiology*, 63(1), 186-193. doi:10.1128/aem.63.1.186-193.1997

Massana, R. (2011). Eukaryotic picoplankton in surface oceans. *Annual Review of Microbiology*, 65, 91-110. doi:10.1146/annurev-micro-090110-102903

Nash, J. D., Kunze, E., Lee, C. M., & Sanford, T. B. (2006). Structure of the Baroclinic tide generated at Kaena Ridge, Hawaii. *Journal of Physical Oceanography*, 36(6), 1123–1135. https://doi.org/10.1175/jpo2883.1

Odebrecht, C., Abreu, P. C., & Carstensen, J. (2015). Retention time generates short-term phytoplankton blooms in a shallow microtidal subtropical estuary. Estuarine, Coastal and Shelf Science, 162, 35–44. https://doi.org/10.1016/j.ecss.2015.03.004

Partensky, F., Hess, W. R., & Vaulot, D. (1999). Prochlorococcus, a Marine Photosynthetic Prokaryote of Global Significance. *Microbiology and Molecular Biology Reviews*, 63(1), 106-127. doi:10.1128/mmbr.63.1.106-127.1999

Pawlowicz, R., Beardsley, B., & Lentz, S. (2002). Classical tidal harmonic analysis including error estimates in MATLAB using T_TIDE. *Computers & Geosciences*, 28(8), 929–937. https://doi.org/10.1016/s0098-3004(02)00013-4

Peterson, J. O., & Peterson, W. T. (2009). Influence of the Columbia River plume on cross-shelf transport of zooplankton. *Journal of Geophysical Research Atmospheres*, 114(C2). https://doi.org/10.1029/2008jc004965

Pugh, D., & Woodworth, P. (2014). Sea-Level Science: Understanding Tides, Surges, Tsunamis and Mean Sea-Level Changes. *Cambridge University Press; Cambridge Core*. https://doi.org/10.1017/cbo9781139235778

Rogers, J. S., Mayer, F. T., Davis, K. A., & Fringer, O. B. (2022). On internal tides driving residual currents and upwelling on an island. *Journal of Geophysical Research Oceans*, 127(7). https://doi.org/10.1029/2021jc018261

Samo, T. J., Pedler, B. E., Ball, G. I., Pasulka, A. L., Taylor, A. G., Aluwihare, L. I., Azam, F., Goericke, R., & Landry, M. R. (2012). Microbial distribution and activity across a water mass frontal zone in the California Current Ecosystem. *Journal of Plankton Research*, 34(9), 802–814. https://doi.org/10.1093/plankt/fbs048

Scanlan, D. J., Ostrowski, M., Mazard, S., Dufresne, A., Garczarek, L., Hess, W. R., Partensky, F. (2009). Ecological Genomics of Marine Picocyanobacteria. *Microbiology and Molecular Biology Reviews*, 73(2), 249-299. doi:10.1128/mmbr.00035-08

Schmidt, K., Birchill, A. J., Atkinson, A., Brewin, R. J. W., Clark, J. R., Hickman, A. E., Johns, D. G., Lohan, M. C., Milne, A., Pardo, S., Polimene, L., Smyth, T. J., Tarran, G. A., Widdicombe, C. E., Woodward, E. M. S., & Ussher, S. J. (2020). Increasing picocyanobacteria success in shelf waters contributes to long-term food web degradation. *Global Change Biology*, 26(10), 5574–5587. https://doi.org/10.1111/gcb.15161

Scotti, A., & Pineda, J. (2007). Plankton accumulation and transport in propagating nonlinear internal fronts. *Journal of Marine Research,* 65(1), 117–145. https://doi.org/10.1357/002224007780388702

Sharples, J., Moore, C. M., & Abraham, E. R. (2001). Internal tide dissipation, mixing, and vertical nitrate flux at the shelf edge of NE New Zealand. *Journal of Geophysical Research Atmospheres*, 106(C7), 14069–14081. https://doi.org/10.1029/2000jc000604

Sharples, J., Tweddle, J. F., Green, J. M., Palmer, M. R., Kim, Y., Hickman, A. E., Holligan, P. M., Moore, C. M., Rippeth, T. P., Simpson, J. H., & Krivtsov, V. (2007). Spring-neap modulation of internal tide mixing and vertical nitrate fluxes at a shelf edge in summer. *Limnology and Oceanography*, 52(5), 1735–1747. https://doi.org/10.4319/lo.2007.52.5.1735

Shelford, E.J., Middelboe, M., Møller, E.F., & Suttle, C.A. (2012). Virus-driven nitrogen cycling enhances phytoplankton growth. Aquatic Microbial Ecology, 66, 1-14. https://doi.org/10.2307/1313569

Sibulan, E.M. and C. S. Acabado. Community structure and dynamics of the picophytoplankton in Batan Bay Estuary [Unpublished data]. College of Fisheries and Ocean Sciences, University of the Philippines Visayas.

Stewart, R. H. (2008). *Introduction to Physical Oceanography* (September 2008). https://oaktrust.library.tamu.edu/bitstream/1969.1/160216/1/stewart_textbook_physical%20oceanography.pdf

Suttle, C. A. (2007). Marine viruses—major players in the global ecosystem. Nature Reviews Microbiology, 5(10), 801–812. https://doi.org/10.1038/nrmicro1750

Takeda, S., Ramaiah, N., Miki, M., Kondo, Y., Yamaguchi, Y., Arii, Y., Gómez, F., Furuya, K., & Takahashi, W. (2007). Biological and chemical characteristics of high-chlorophyll, low-temperature water observed near the Sulu Archipelago. *Deep Sea Research Part II Topical Studies in Oceanography*, 54(1–2), 81–102. https://doi.org/10.1016/j.dsr2.2006.08.020

The MathWorks Inc. (2024). MATLAB version: 24.2.0.2712019 (R2024b). Retrieved from Natick, Massachusetts: The MathWorks Inc.

Thomson, R. E., & Emery, W. J. (2014). *Data Analysis Methods in Physical Oceanography*. Elsevier Science.

Wilhelm, S.W., & Suttle, C.A. (1999). Viruses and nutrient cycles in the sea. BioScience, 49(10), 781-788. https://doi.org/10.3354/ame01553

Wunsch, C. (1996). *The ocean circulation inverse problem*. https://doi.org/10.1017/cbo9780511629570

Xie, D., Feng, C., Hu, J., Lin, H., Luo, H., Zhang, Q., & He, H. (2024). Impact of tidal fluctuations on bacterial community structure in Wuyuan Bay: A comparative analysis of waters inside and outside the tidal barrage. PLoS ONE, 19(10), e0312283. https://doi.org/10.1371/journal.pone.0312283

Xing, J., & Davies, A. M. (2011). On the interaction of internal tides over two adjacent sills in a fjord. *Journal of Geophysical Research Atmospheres*, 116(C4). https://doi.org/10.1029/2010jc006333

Yu, Y., Xing, X., Liu, H., Yuan, Y., Wang, Y., & Chai, F. (2019). The variability of chlorophyll-a and its relationship with dynamic factors in the basin of the South China Sea. Journal of Marine Systems, 200, 103230. https://doi.org/10.1016/j.jmarsys.2019.103230

Date received: September 30, 2025 *Date accepted: February 13, 2026*

Authors:

Edcel R. Sudaria, Institute of Marine Fisheries and Oceanology, College of Fisheries and Ocean Sciences, University of the Philippines Visayas, Miagao (5023), Iloilo; email: ersudaria@up.edu.ph

Gency L. Guirhem-Helican, Institute of Marine Fisheries and Oceanology, College of Fisheries and Ocean Sciences, University of the Philippines Visayas, Miagao (5023), Iloilo; email: glguirhem@up.edu.ph

Richard N. Muallil, Mindanao State University- Tawi Tawi, College of Technology and Oceanography, Sanga-Sanga, Bongao, Tawi-Tawi, Philippines (7500); email:rnmuallil@msutawi-tawi.edu.ph

Charina Lyn Amedo. Repollo, Marine Science Institute, College of Science, University of the Philippines Diliman, Quezon City, Philippines, (1101); email: crepollo@msi.upd.edu.ph

Cristy S. Acabado, Institute of Marine Fisheries and Oceanology, College of Fisheries and Ocean Sciences, University of the Philippines Visayas, Miagao (5023), Iloilo; email: csacabado@up.edu.ph